The 2010 IEEE/RSJ International Conference on
Intelligent Robots and Systems
October 18-22, 2010, Taipei, Taiwan

Empirical Based Optimal Design of Active Strobe Imager

Kohei Funai, Koji Mizoue, Mitsuru Higashimori, Kenjiro Tadakuma and Makoto Kaneko

***Abstract*— We discuss an empirical based design of Active Strobe Imager(ASI) that enables us to visualize the dynamic behavior of tissue, even under a high frequency vibration that cannot be followed by the naked eye. A pneumatic actuator imparts a vibration for the target object. By flashing light with slightly different frequency, we can see the dynamics by the naked eye. We discuss an approach for determining a set of optimal parameters of ASI by considering both the uncomfortability sensation due to light flickering, the sharpness of the motion, and the amplitude of the vibration of the object. We also give an example of optimal parameter determination for human skin.**

I. INTRODUCTION

The recognition speed of human eye is limited in the frequency range of less than 15[Hz]. Due to this, human eye cannot follow the object vibration whose frequency is more than 15[Hz]. In order to visualize such a high frequency vibration, there is a well-known technique where a strobe with slightly different flashing frequency is utilized. This is a very powerful approach for visualizing the object vibration by our naked eye; otherwise there is no chance to see it in real time. There have been two well-known application fields; one is for confirming the rotational speed of mechanical systems when there is no velocity sensor available, the other is for examining a larynx by visualizing with strobe with appropriate flashing frequency. The system is called "stroboscopy" [1], [2]. For both cases, objects are vibrating by themselves. On the other hand, there is a particular application where the concerned object is in stationary state and the object vibration is compulsorily generated by an external actuator. As for the second application, we have proposed "Active Strobe Imager (ASI)" [3] where a pulsated air puff is actively imparted to human lung with tumors, and with an assistance of strobe light with slightly different flashing frequency, the system enables us to visualize clearly where tumors are. This imager directly shows what is really happening without converting into numerical value using an appropriate software developed by engineers. Medical doctors would judge for a further treatment by direct observation through his/her own eye. In this sense, ASI gets a good reputation, especially from medical doctors.

This paper discusses an extended version of ASI. The key design is to implement both optical and pneumatic systems into one package, so that we can easily handle it by releasing from the difficulty of coordinating individual systems. We also take the concept of a common-axis type imager where both optical and pneumatic axes are identical each other. With this design, both light flashing and air puff can be easily focused on the object. Fig. 1 shows an overview of the newly developed ASI, where (a) and (b) are the side view and the frontal view, respectively. In order to make ASI work adequately, we have to set the parameters controlling the system performance in a proper state. Under the given hardware, we discuss an empirical based optimal design of parameters, such as the frequency of pulsated air, the frequency of light flashing, and the duty factor indicating the on-time over time period in light flashing, by considering the uncomfortability level due to flickering coming from the light switching and the sharpness of motion picture and the amplitude of the vibration of the object.

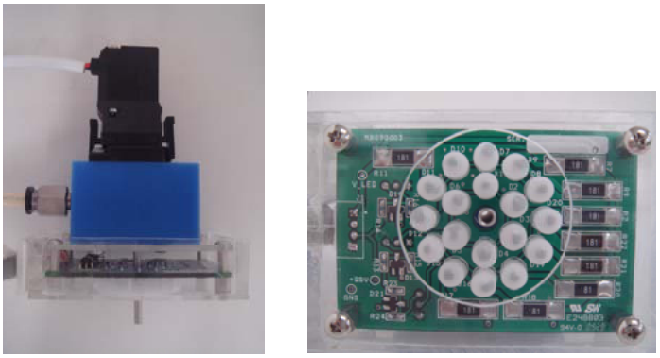

(a) Side view (b) Frontal view

Fig. 1. An overview of a common-axis type ASI

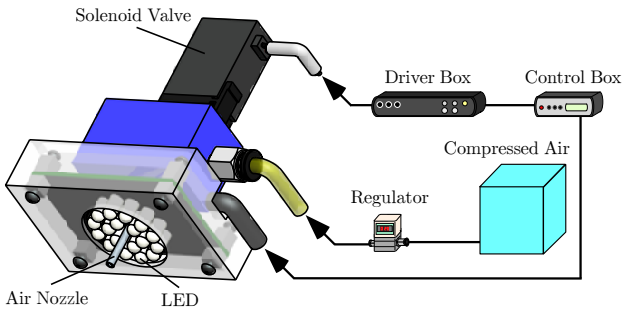

Fig. 2. An overview of the whole system

K. Funai, M. Higashimori, K. Tadakuma and M. Kaneko are with the Department of Mechanical Engineering, the Graduate School of Engineering, Osaka University, 1-1 Yamadaoka, Suita, Osaka, 565-0871, JAPAN. K. Mizoue is with MIZOUE PROJECT JAPAN Corporation, 1-305, Takagicho, Fuchu, Hiroshima, 726-0013, JAPAN. funai@hh.mech.eng.osaka-u.ac.jp, {higashi, tadakuma, mk}@mech.eng.osaka-u.ac.jp, president@mizoueproject.com

This paper is organized as follows. After reviewing related works in chapter 2, we explain the composition and basic working principle of ASI in chapter 3. In chapter 4, we discuss an empirical based optimal parameter determination of ASI. In chapter 5, we give an example of optimal parameter determination for human skin before concluding this work in chapter 6.

II. Related Works

ASI is categorized into active sensing, where we impart a force into an object and observe what happens. As for active sensing, there are two approaches; one is the direct approach where a force is given to the object directly through a contact probe [4]-[8], and the other is the indirect approach where a force is given to the object indirectly through a fluid force [9]-[14]. As a fluid force, either an air puff or a water jet is often utilized. We have focused on indirect approach, since an air puff can impart a gentle force to a tissue, while a direct approach based on tactile probe often brings about a serious issue due to the interaction force between the probe and the environment. A contact through air puff is really meaningful from the viewpoint of avoiding any damage to human body. Also, since an air puff based approach is transparent, there is no concern about the probe occluding the target object. Most of indirect approaches have been, therefore, applied for medical fields, such as diagnosis of eye stiffness measurement [11], stomach [12], lung [13], skin [14], [15] and so forth. In direct and indirect approaches, either a distance sensor or a vision sensor is usually implemented for detecting the deformation profile of the imparted force, while ASI does not include any sensor. Instead of distance sensors, human can directly observe the scene that cannot be seen without ASI. In esthetic fields, various sensing probes [16] have been developed for evaluating the skin age with a numerical value, but seeing is really believing while converting a sensing value into an age does not make much sense.

III. The Composition and Basic Working Principle of ASI

Fig. 2 shows an overview of ASI composed of a couple of components, such as a high speed solenoid valve for imparting a pulsated force to the object to be tested, an air compressor for providing a pressed air to the nozzle, a strobe system for supplying periodic flashing light, and a computer for controlling all of them appropriately. It is usually hard for us to bring all those equipments for testing as well as setting up due to their separate components. Here, we propose a common-axis type ASI with tuning free in opto-pneumatic hybrid arrangement, as shown in Fig. 1, where LEDs implemented around the air nozzle are designed so that both optical and pneumatic systems may have a common axis. This mechanical configuration is greatly convenient for testing, since we are completely released from tuning both optical and pneumatic axes during measurement. The ASI is controlled by a couple of important parameters, such as air pressure p in the air regulator, the frequency of air puff f_{a},

Fig. 3. Four components of electro-magnetic valve

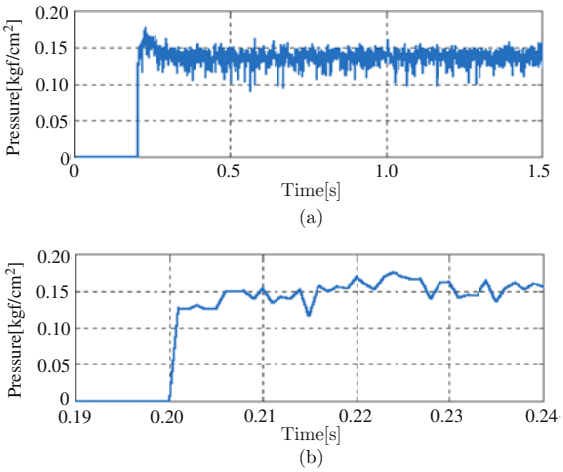

Fig. 4. Step response of air-jet system

the frequency of the light flashing f_{s}, and the duty factor. The duty factor is defined by

$$\alpha = \frac{T_{\mathrm{on}}}{T_{\mathrm{on}} + T_{\mathrm{off}}} \tag{1}$$

where T_{on} and T_{off} are the on-time and the off-time, respectively. We have to consider two different duty factors, namely α_{a} and α_{s}, where the subscripts "a" and "s" denote "air" and "strobe", respectively. All control parameters except p can be set up by a PC through a RS-232C cable connection as well as by potentiometers equipped in the control box. Fig. 3 shows the electro-magnetic based pneumatic valve. As you can see, the mechanical components are simple enough to guarantee its easy maintenance. The valve does not have any mechanical spring so that we can reduce the number of components. Instead of such a spring, this valve utilizes the force due to the back pressure coming from the air tank, while the active force is produced by an electro-magnetic force. Fig. 4 shows the step response, where (a) and (b) are shown with different time scale. The pressure is measured by using a pressure sensor implemented at a distance of 2[cm] from the nozzle. As we can see from Fig. 4, the step response is quick enough to ensure that the time constant is within 1[ms]. This may actually be a bit overspecification for applying ASI. Other important mechanical specification is the length of nozzle and the position of LEDs. As for

the nozzle length, we cannot get a quick response due to the compressibility of air, if we take a long nozzle. By considering this effect, we choose the length of 50[mm]. As for the position of LEDs, there are two further concerns; one is the distance between the face of nozzle and the LED plane, and the other is the density of LED, namely, how many LEDs for unit area. We usually utilize an ASI keeping roughly a 10∼20[mm] distance between the nozzle face and the object to be tested. Through a preliminary experiment, we found that the distance between the LED plane and the object is roughly 20∼40[mm] for proper operation. Suppose that a pulsated air puff with a frequency of f_a. We also suppose that this frequency is beyond the recognition speed of human eye. While human cannot recognize the vibration at all under such a condition, we can observe the object in every flashing point, as a result we can see the object as if it were vibrating with a virtual frequency of $f_v = |f_a - nf_s|$ where n is a positive integer. In case of a soft tissue, we can also observe a wave moving toward the inward direction under $f_a - nf_s < 0$, while the wave is moving the outer direction under $f_a - nf_s > 0$. When we make the sinusoidal wave with the frequency of f_a , by using AD converter with the sampling rate of f_s, the captured signal includes the sinusoidal wave with the virtual frequency of $|f_a - nf_s|$. In the case of ASI, if f_s and f_a are close each other, namely $|f_a - nf_s|$ is roughly less than 5[Hz], we can observe the sinusoidal signal with the frequency of $|f_a - nf_s|$ by our naked eye. This phenomenon is called aliasing in signal processing field. The working principle of ASI is exactly the same as that of aliasing. As for light flashing, we utilize a set of 18 white LEDs instead of a strobe scope toward a compact design. This choice is good from the viewpoint of power saving as well as the miniaturized design.

IV. Optimal Parameter Determination

Suppose f_h to be the maximum frequency where we can visually observe the oscillation by the naked eye. Through the discussion in chapter 3, we have to keep the following condition

$$|f_v| \leq f_h \tag{2}$$

Focusing on the wave spreading toward the outer direction, eq. (2) results in

$$0 < f_a - nf_s \leq f_h \tag{3}$$

Generally, we can keep the highest visual resolution for $n = 1$, and the resolution goes down, as n increases. By this reason, we keep $n = 1$ hereafter. As a result, eq. (3) is rewritten by

$$0 < f_a - f_s \leq f_h \tag{4}$$

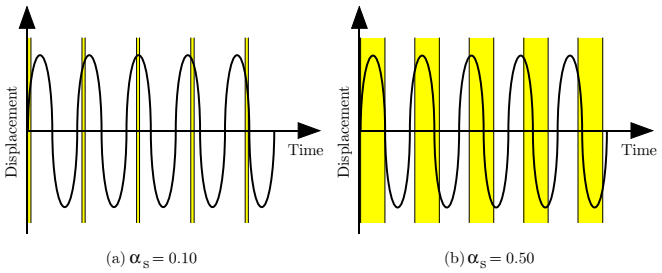

Fig. 5. The relationship between α_s and the phase of LED flashing

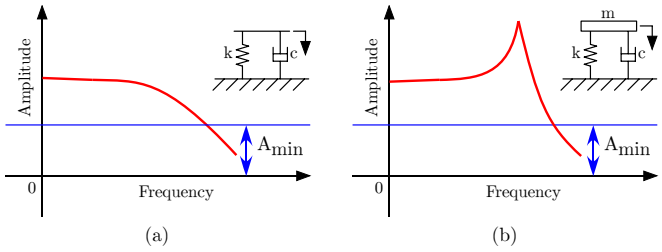

Fig. 6. An example of the relationship between frequency and amplitude

Empirically, it is well known that our eye naturally follows the motion under a low virtual frequency. Based on this fact, we choose $f_v = 1$, and eq. (4) is further rewritten as

$$f_a - f_s = 1 \tag{5}$$

where we implicitly suppose that both f_a and f_s are positive integer. Eq. (5) means that f_a and f_s are coupled each other. Hereafter, we consider three parameters α_a, α_s, and f_a (or f_s). Now, we further break down "clear observation of object motion by the naked eye" into three keywords.

Condition (1): Avoiding flickering
Condition (2): Sharpness of motion
Condition (3): Amplitude of vibration of object

As f_s decreases, our eye starts to recognize the light flashing, especially when f_s is close to f_h. Under such a condition, our eye is not comfortable and it is hard to continuously observe the object motion. Such a flickering can be easily avoided by increasing f_s. The condition (1) can be written by the following condition

$$f_{sb} \leq f_s \tag{6}$$

where f_{sb} is the minimum frequency where our eye can see the object motion without flickering.

Now let us consider the condition (2). As for lighting, it is well known that a clear strobe picture is obtained under small duty factor as shown in Fig. 5(a) and a clear picture cannot be obtained under a large duty factor as shown in Fig.

5(b). This is because a clear picture is obtained under less overlapping between lights flashing, as shown in Fig. 5(a). We now define $\alpha_{\text{s-dis}}$ as the maximum α_{s} where the object motion is sharply observed. On the other hand, it is really hard to catch the motion of the object under too little lighting condition, which means that we need a minimum duty factor $\alpha_{\text{s-min}}$, unless the system has an adaptive tuning function for the light strength. These discussions result in the following condition for α_{s}

$$\alpha_{\text{s-min}} \leq \alpha_{\text{s}} \leq \alpha_{\text{s-dis}} \tag{7}$$

Finally, let us consider the condition (3). Intuitively, a larger amplitude is better from the viewpoint of obtaining a clear observation by our naked eye. For example, suppose two different object models, as shown in Fig. 6, where (a) and (b) are a spring-damper model and a spring-mass-damper model, respectively. It is well known that human skin behaves just like a spring-damper model for a given periodic force. The amplitude of the object is a function of both f_{a} and α_{a}, namely $A = A(f_{\text{a}}, \alpha_{\text{a}})$. We would decide f_{a} and α_{a} in such a way that A may be maximized. But we cannot determine f_{a} alone because f_{a} is coupled with f_{s}. So, we define the range of the value where A can be taken. Now, we suppose the minimum observable amplitude A_{min} by the naked eye. Under A_{min}, we have to keep the following constraint

$$A_{\text{min}} \leq A(f_{\text{a}}, \alpha_{\text{a}}) \tag{8}$$

We now define our optimum problem as follows

Find $\hat{\alpha_{\text{a}}}$, $\hat{\alpha_{\text{s}}}$ and $\hat{f}_{\text{a}}$ to maximize A.
subject to: $f_{\text{sb}} \leq f_{\text{s}}$
$\alpha_{\text{s-min}} \leq \alpha_{\text{s}} \leq \alpha_{\text{s-dis}}$
$A_{\text{min}} \leq A(f_{\text{a}}, \alpha_{\text{a}})$

We note that f_{sb}, $\alpha_{\text{s-min}}$, $\alpha_{\text{s-dis}}$ and A_{min} can be obtained only through experiments. Therefore, we cannot obtain a set of optimum parameters without fixing an object. We note that it is not guaranteed whether this problem can be solved mathematically or not, since it may strongly depend on the characteristics of the object.

V. Optimum parameters for human skin

In order to determine a set of optimum parameters, we pick up human skin in this chapter. Fig. 7 shows an example of human skin behavior under a periodic flashing light with a frequency of 60[Hz]. For this example, we find a set of optimum parameters, $\hat{\alpha_{\text{a}}}$, $\hat{\alpha_{\text{s}}}$ and $\hat{f}_{\text{a}}$, where the hat "^" denotes an optimum value.

A. f_{sb}

We executed experiments to find f_{sb} for 10 subjects whose ages are between 22 through 26. We make f_{s} decrease gradually with a step of 5[Hz] from 100[Hz] until a subject eventually loses the existense of wave due to flickering. Fig. 8 shows the experimental results for 10 subjects, where each point denotes the lower boundary of f_{s} where each subject feels heavily flickering. While the lower boundary, of course, depends on subjects, all subjects could clearly observe the object vibration with $f_{\text{s}} \geq 60$[Hz]. As a result, we set $f_{\text{sb}} = 60$[Hz]. We would note that these flickering data are nicely coincident with former works [17], [18].

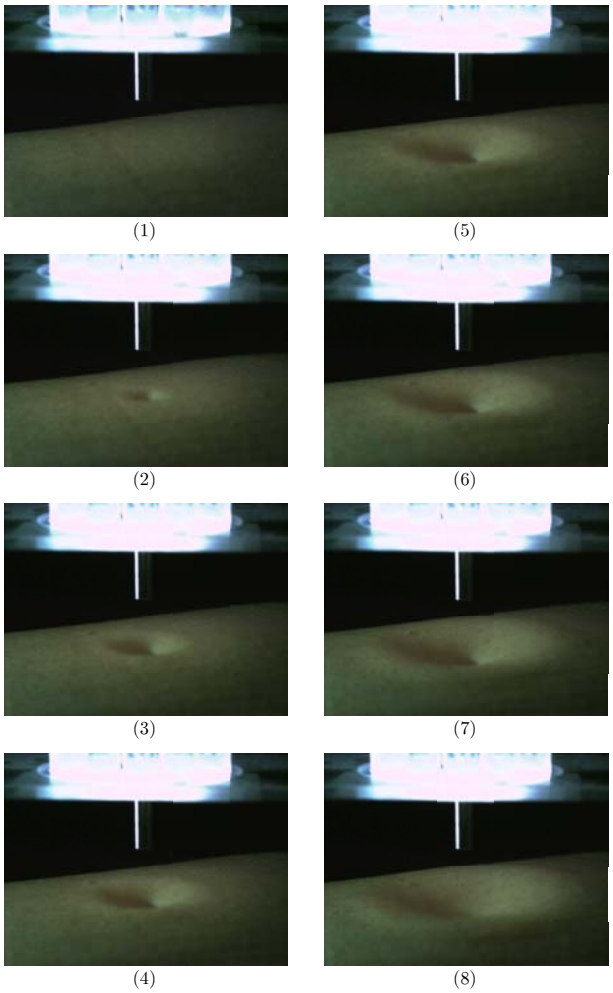

Fig. 7. Observation of human skin; these pictures were captured using a different light source in addition to LEDs implemented in the ASI, so that we can obtain clear set of pictures.

B. $\alpha_{s\text{-}min}$ and $\alpha_{s\text{-}dis}$

In order to determine $\alpha_{\text{s-min}}$ and $\alpha_{\text{s-dis}}$, we executed the experiment where each subject answers α_{s} making him/her feel with the most clear picture through his/her naked eye. Fig. 9 shows the experimental results. From Fig. 9, we can see that good conditions are given for α_{s} = 0.10 and 0.15. As a relaxed condition, we obtain $0.05 \leq \alpha_{\text{s}} \leq 0.20$ for providing a sharp lighting condition, and as a result, we set $\alpha_{\text{s-min}} = 0.05$ and $\alpha_{\text{s-dis}} = 0.20$.

C. A_{min}

Fig. 10 shows the amplitude of skin for various f_{a} and α_{a}. From Fig. 10, we can see that the amplitude under

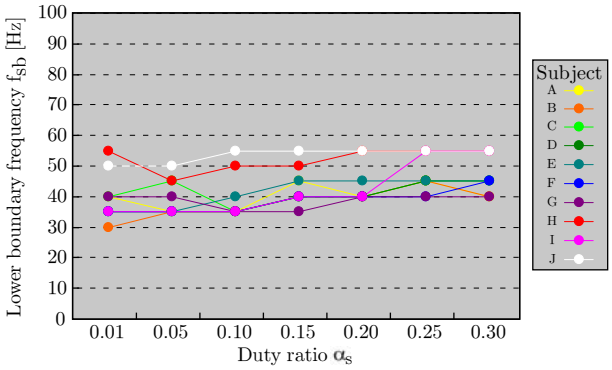

Fig. 8. Lower boundary frequency of each subject

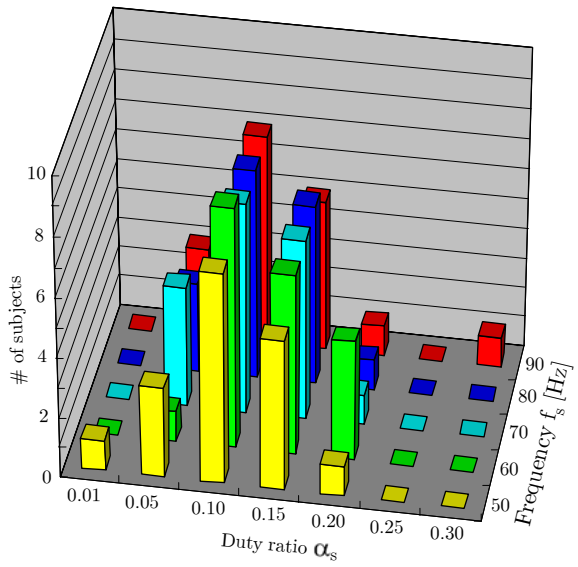

Fig. 9. The relationship among f_s, α_s and the # of subjects feeling satisfaction

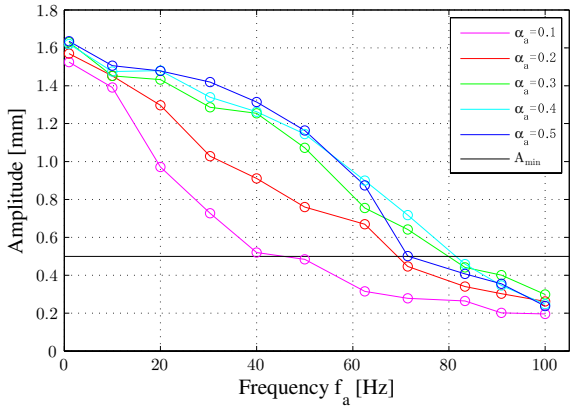

Fig. 10. The relationship between air frequency and amplitude

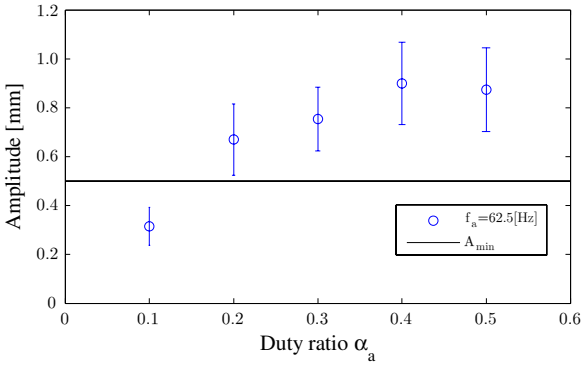

Fig. 11. An example of amplitude average and standard deviation

constant α_a gradually decreases with respect to f_a without any resonance point and this is a typical behavior of spring-damper model. Fig. 11 shows the average amplitude and the standard deviation for various α_a, under $f_a = 62.5$[Hz]. Through this experiments, we found that we can observe the skin behavior whose minimum amplitude is A_{min} = 0.5[mm], which is indicated in the real line in Fig. 10.

D. Determination of optimum parameters

Let us consider a 3D space where f_a, α_a and α_s span orthogonally, as shown in Fig. 12. The flickering condition, the condition for obtaining a clear picture, and the condition for guaranteeing the minimum amplitude are given by the space in [i], [ii] and [iii], respectively. We note that the space in [iii] is modeled by a polygon. The common space [iv] for all spaces [i], [ii] and [iii] is given in Fig. 12(b), while all spaces are given in Fig. 12(a). It is still not that easy to obtain the optimal solution from the common space [iv]. Now, let us come back to Fig. 9. From Fig. 9, we find that $\alpha_s = 0.10$ is the best parameter for α_s in terms of obtaining a sharp picture by our naked eye. By considering this fact, we focus on the constraint space in the cross section of $\alpha_s = 0.10$. This cross section is given in Fig. 12(c). As the amplitude decreases with the increase of f_s, we should choose the smallest f_s, namely $\hat{f}_s$ = 60. Since $\hat{f}_a - \hat{f}_s = 1$, $\hat{f}_a = \hat{f}_s + 1 = 61$[Hz]. From Fig. 12(c), the optimum condition exists along the line segment given by f_a = 61[Hz]. Now, let us come back to Fig. 10. The maximum amplitude is given by $\alpha_a = 0.4$ under f_a = 61[Hz]. However, since there is no real difference of amplitude between $\alpha_a = 0.3$ and $\alpha_a = 0.5$, we choose $\hat{\alpha}_a$ = 0.3 from the viewpoint of avoiding damage to the object due to a large applied force. The movie which was taken under the optimum set of parameters is available in the webcite [19].

While the approach leading to the solution is not so beautiful from the viewpoint of mathematics, we can eventually reach it step by step by considering the empirical data. We would also note that if the object is replaced by another one, f_s and α_s do not change significantly, because these parameters depend on human eye, and that since the dynamic

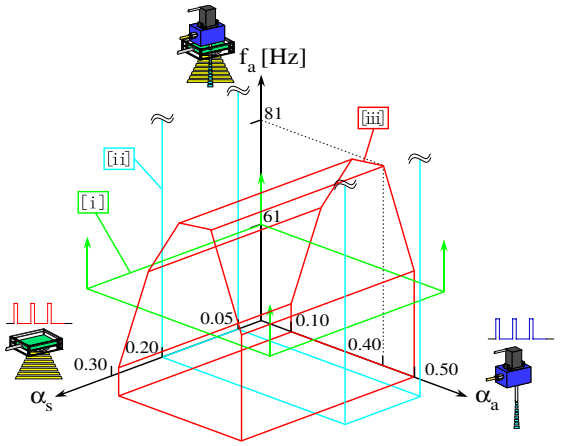

(a) Constraint space

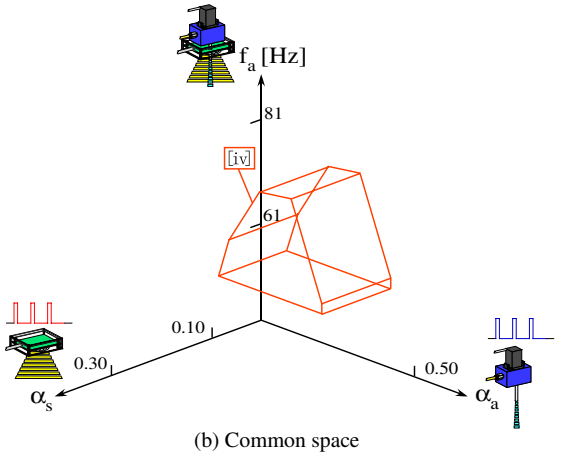

(b) Common space

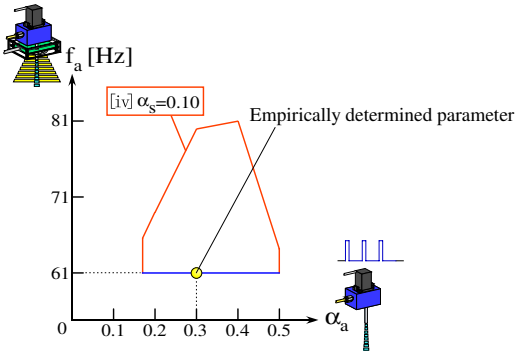

(c) Optimum point

Fig. 12. Constraint space

parameters such as damping factor and stiffness do not heavily change from subject to subject, it is not necessary to change the optimal parameters after we obtained them once.

VI. Concluding Remarks

We discussed a common-axis type ASI. What we have done in this paper can be summarized as follows;

- We proposed a common-axis type ASI, where both optical and air nozzle axes coincide each other and explained its advantageous points compared with the conventional one.
- We introduced an optimal determination of parameters of ASI, especially for the frequency of pulsated air puff, the duty factor for lightening, and the duty factor for air puff, by considering the incomfortability of flickering due to light switching, the clearness of picture by the naked eye and the amplitude of the vibration of the object.

For a future work, we are planning to release the developed ASI in the esthetic and medical markets.

Finally, this work is partially supported by g-COE "in-Silico Medicine (Osaka University)".

References

[1] S. Saito, H. Fukuda, H. Ono, and Y. Isogai, "Observation of vocal fold vibration by x-ray stroboscopy," *The Journal of the Acoustical Society of America*, 64, pp. S90–S91, 1978.

[2] N. Weir and I. Bassett, "Outpatient fibreoptic nasolaryngoscopy and vidostroboscopy," *Journal of the Royal Society of Medicine*, 80, pp. 299–300, 1987.

[3] M. Kaneko, C. Toya, and M. Okajima, "Active Strobe Imager for Visualizing Dynamic Behavior of Tumors," *Proc. of the 2007 IEEE International Conf. on Robotics and Automation*, pp. 3009–3014, 2007.

[4] P.S. Wellman and R.D. Howe, "Modeling Probe and Tissue Interaction for Tumor Feature Ectraction," *1997 ASME Summer Bioengineering Conference*, 35, pp. 237–238, 1997.

[5] P. S. Wellman, E. P. Dalton, D. Krag, K. A. Kern, R. D. Howe, "Tactile Imaging of Breast Masses: First Clinical Report," *Arch Surg*, vol. 136, pp.204–208, 2001.

[6] J. Dargahia, S. Najarianb and B. Liua, "Sensitivity analysis of a novel tactile probe for measurement of issue softness with applications in biomedical robotics," J. of Materials, Processing Technology, vol. 128, pp. 176–182, 2007.

[7] Y. Kurita, R. Kempf, Y. Iida, J. Okude, M. Kaneko, H. K Mishima, H. Tsukamoto, E. Sugimoto, S. Katakura, K. Kobayashi, and Y. Kiuchi, "Contact Based Stiffness Sensing of Human Eye," *IEEE Transactions on Biomedical Engineering*, vol. 55, No. 2, pp. 739–745, 2008.

[8] H. Goldmann, F.W. Nwell, Ed., "Applanation tonometry," *in Trans. 2nd Conf. Glaucoma*, New York, pp. 167–220. 1957.

[9] Y. -C. Ko, C.-I. Liu, W. -M. Hsu, "Varying effect of corneal thickness on intraocular pressure measurement with different tonometers," *Eye*, pp. 1–6. 2004.

[10] K. Damji, R. Muni, R. Munger, "Influence of corneal variables on accuracy of intraocular pressure measurement," *J. Glaucoma*, vol. 12, pp. 69–80, 2003.

[11] M. Kaneko, R. Kempf, Y. Kurita, Y. Iida, H. K Mishima, H. Tsukamoto, and E. Sugimoto, "Measurement and Analysis of Human Eye Excited by an Air Pulse," *IEEE International Conference on Multisensor Fusion and Integration for Intelligent Systems (MFI 2006)*, TuB02.5, Heidelberg, Germany, Sep. 2006.

[12] M. Kaneko, T. Kawahara, S. Matsunaga, T. Tsuji, and S. Tanaka, "Touching Stomach by Air," *IEEE Proceedings of International Conference on Robotics and Automation*, pp. 644–669, 2003.

[13] T. Kawahara, C. Toya, N. Tanaka, M. Kaneko, Y. Miyata, M. Okajima, and T. Asahara, "Non-Contact Impedance Imager with Phase Differentiator," *an Proc. of the 1st IEEE/RAS-EMBS Int. Conf. on Biomedical Robotics and Biomechatronics*, paper no. 159, 2006.

[14] N. Tanaka, M. Higashimori, and M. Kaneko, "Active Sensing for Viscoelastic Tissue with Coupling Effect," *30th Annual International Conference of the IEEE Engineering in Medicine and Biology Society (EMBC 2008)*, Vancouver, Canada, pp. 106–111, 2008.

[15] F. Lacquanti, F. Licata and J. F. Soechting, "The mechanical behavior of the human forearm in response to transient perturbations," *Biological Cybern*, vol. 44, pp. 35–46, 1982.

[16] http://www.skintechonline.com/lamprobe_faq.htm

[17] J. E. Farrell, Brian L. Benson and Carl R.Haynie "Predicting flicker thresholds for video display terminals," *Proceedings of the Society for Information Display*, vol. 28, No. 4, pp. 449–453, 1987.

[18] D. Bauer, "Use of slow phosphors to eliminate flicker in VDUs with bright background," *Displays*, vol. 8, Jan, pp. 29–32, 1987.

[19] http://www-hh.mech.eng.osaka-u.ac.jp/sensing/asi_e.html